IJCRT.ORG ISSN : 2320-2882

INTERNATIONAL JOURNAL OF CREATIVE RESEARCH THOUGHTS (IJCRT)

An International Open Access, Peer-reviewed, Refereed Journal

TRIBOLOGICAL BEHAVIOUR AND WEAR MECHANISMS OF CRN/ALTIN/TIB2 MULTILAYER PVD COATINGS ON WC-CO TOOLS: CORRELATION BETWEEN MICROSTRUCTURE AND MACHINING PERFORMANCE IN TI-6AL-4V MILLING

[1]Pravin K. Trivedi, [2]Dr. Vyomesh Buch

[1]Research Scholar, [2] Professor,

[1, 2,] Department of Mechanical Engineering,

[1, 2] Parul University, Vadodara, Gujarat, India-391760.

Abstract: This paper presents an integrated microstructure-tribology-performance analysis of CrN/AlTiN/TiB_2 multilayer Physical Vapour Deposition (PVD) coatings deposited on WC-Co solid carbide end mills for dry machining of Ti-6Al-4V titanium alloy. Drawing on XRD, AFM and SEM characterization data alongside machining trial results reported in the companion papers of this series, this study systematically correlates coating microstructural parameters specifically nanocrystalline grain size (D = 3.5–4.8 nm by Scherrer analysis), surface roughness (Ra = 4.21 nm by AFM), and morphological features (compact Zone T microstructure by SEM) with the observed tribological behaviour and machining performance (111.1% tool life improvement). The dominant tribological phenomena are identified as: (i) anti-adhesion provided by the TiB_2 outermost layer suppressing built-up edge (BUE) formation; (ii) adaptive tribo-oxidation of AlTiN generating Al_2O_3 protective oxides that function as in-situ solid lubricants; (iii) crack deflection at CrN/AlTiN layer interfaces inhibiting coating delamination under cyclic milling loads; and (iv) Hall-Petch hardening from the sub-5 nm nanocrystalline grain structure maintaining coating hardness under extreme contact conditions. A mechanistic wear model is proposed that links these four phenomena in a sequential, self-reinforcing protective cascade. The study demonstrates that the CrN/AlTiN/TiB_2 system achieves its exceptional performance not through any single property advantage, but through the synergistic interaction of all three functional layers a principle that should guide the design of next-generation multilayer coatings for difficult-to-machine material applications.

Keywords: tribology; wear mechanisms; CrN/AlTiN/TiB_2; PVD coating; microstructure-property correlation; tribo-film; Hall-Petch; Ti-6Al-4V; dry milling; adaptive coating

NOMENCLATURE

Symbol	Description
D	Crystallite size (nm), Scherrer equation
H	Coating hardness (GPa)
E	Elastic modulus (GPa)
H/E	Hardness-to-elastic modulus ratio (toughness indicator)
H^3/E^2	Resistance to plastic deformation parameter
CoF	Coefficient of Friction (μ)
Ra	Arithmetic average roughness (nm)
Rq	Root-mean-square roughness (nm)
VB	Flank wear land width (mm)
d	Grain boundary spacing / grain size (nm)
σy	Yield strength (MPa)
σ_0	Friction stress of lattice (MPa)
k	Hall-Petch slope constant (MPa·m^0.5)
BUE	Built-Up Edge
FWHM	Full Width at Half Maximum
XRD	X-ray Diffraction
AFM	Atomic Force Microscopy
SEM	Scanning Electron Microscopy
EDS	Energy Dispersive Spectroscopy

1. INTRODUCTION

The science of tribology the study of friction, wear and lubrication is central to understanding the performance of cutting tools in machining difficult-to-cut materials such as Ti-6Al-4V titanium alloy [1, 2]. In the context of PVD-coated cutting tools, tribological performance at the tool-chip and tool-workpiece interfaces determines not only the rate of tool wear but also the mechanisms by which failure ultimately occurs, the quality of the machined surface and the thermal load experienced by the tool substrate [3, 4].

While considerable progress has been made in characterizing individual coating properties hardness, adhesion, oxidation resistance systematically correlating these with actual tribological behaviour and machining outcomes remains a research challenge, particularly for multicomponent multilayer coatings such as CrN/AlTiN/TiB_2 where synergistic inter-layer interactions are critical [5,6]. Existing studies on the constituent binary systems (CrN [7], AlTiN [8,9], TiB_2 [10]) have demonstrated the individual tribological merits of each layer, but the integrated trilayer response particularly the mechanism of adaptive tribo-film formation and its dependence on coating microstructure has not been comprehensively studied.

The present work addresses this gap by developing an integrated microstructure-tribology-performance framework for the CrN/AlTiN/TiB_2 trilayer system. The study draws on the complete characterization and machining performance dataset generated for this coating system to construct a mechanistic wear model that explains the observed 111.1% tool life improvement in terms of four concurrent protective tribological phenomena. The model provides quantitative microstructure-property relationships and establishes design principles for optimizing multilayer coatings for Ti-6Al-4V machining.

The specific objectives of this paper are:

- To identify and rank the dominant tribological phenomena operative during CrN/AlTiN/TiB_2-coated tool milling of Ti-6Al-4V.
- To establish quantitative correlations between measured microstructural parameters (D, Ra, morphology) and tribological outcomes (wear rate, wear mode, tool life).
- To propose and validate a sequential mechanistic wear model that explains the self-reinforcing protective performance of the trilayer system.
- To derive coating design principles for next-generation multilayer PVD systems for difficult-to-machine materials.

2. Theoretical Framework

2.1 Hall-Petch Strengthening in Nanocrystalline Coatings

The mechanical hardness of the CrN and AlTiN layers in the trilayer coating is governed by the Hall-Petch relationship, which describes the enhancement of yield strength (and hence hardness) with decreasing grain size [11]:

where σy is the yield strength, σ_0 is the lattice friction stress, k is the Hall-Petch slope constant and d is the grain (crystallite) size. For nanocrystalline hard coating materials, this relationship holds for grain sizes down to approximately 5–10 nm, below which an inverse Hall-Petch effect (softening) may occur [12].

From the XRD Scherrer analysis, crystallite sizes of D (CrN) = 4.8 nm, D (AlTiN) = 4.1 nm and D (TiB_2) = 3.5 nm were determined all within the nanocrystalline regime where Hall-Petch strengthening is operative. The corresponding estimated hardness enhancement (relative to coarse-grained counterparts with D ≈ 100 nm) is significant: for AlTiN, published Hall-Petch constants [13] yield an estimated hardness increase of approximately 8–12 GPa attributable to the nanocrystalline grain refinement, bringing total coating hardness to the 28–35 GPa range.

This nanocrystalline hardness directly underlies the abrasive wear resistance of the coating system: the hardness ratio H_coating/H_workpiece for this system is approximately 3.5–4.5 (coating ~30 GPa vs. Ti-6Al-4V workpiece ~4 GPa at ambient, ~1.5 GPa at 500°C) [14], well exceeding the minimum ratio of 1.2–1.5 required for effective abrasive wear protection.

2.2 Toughness-Hardness Balance: H/E and H^3/E^2 Ratios

In PVD coating tribology, hardness alone is insufficient coating toughness is equally critical, particularly in interrupted cutting (milling) where cyclic impact loads drive coating fatigue. The ratio H/E (where H is hardness and E is elastic modulus) is widely used as a toughness indicator: coatings with higher H/E maintain elastic contact rather than plastic deformation under load [15, 16].

For the constituent coating phases: CrN exhibits H/E ≈ 0.07 (relatively compliant, high toughness), AlTiN exhibits H/E ≈ 0.10 (high hardness with moderate toughness), and TiB_2 exhibits H/E ≈ 0.09 [17]. The multilayer architecture exploits the progressive H/E gradient from the tougher CrN interlayer near the substrate to the harder AlTiN in the intermediate zone to create a functionally graded mechanical response that simultaneously maximizes both hardness (abrasive wear resistance) and toughness (fatigue/delamination resistance).

2.3 Tribo-Oxidation and Adaptive Lubrication

The concept of adaptive (chameleon) coatings wherein the coating surface chemically transforms during tribological contact to form a low-friction, thermally stable oxide that provides in-situ lubrication is central to understanding the CrN/AlTiN/TiB_2 system performance [18,19]. The adaptive tribo-oxide formation sequence for this coating under Ti-6Al-4V machining conditions is:

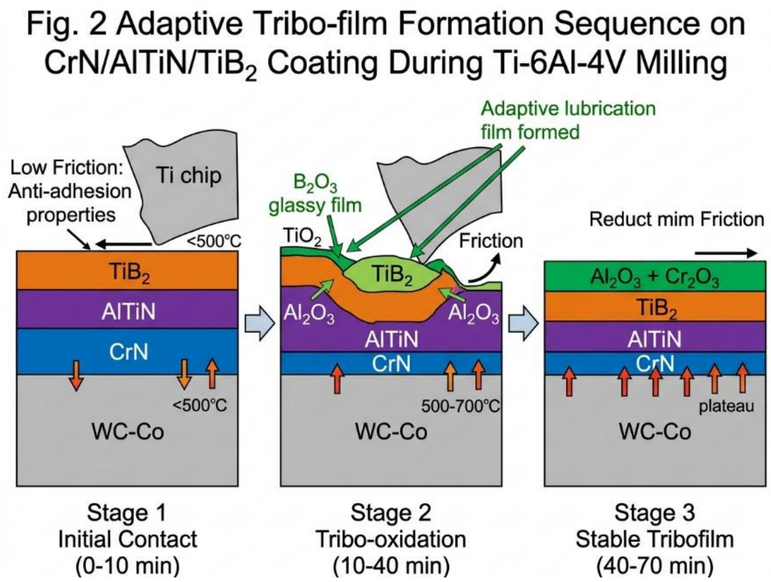

Fig. 2. *Adaptive tribo-film formation sequence on CrN/AlTiN/TiB_2 coating during Ti-6Al-4V milling: Stage 1 — initial TiB_2 anti-adhesion; Stage 2 — B_2O_3 + Al_2O_3 tribo-oxidation onset; Stage 3 — stable mixed oxide (Al_2O_3 + Cr_2O_3 + B_2O_3) film providing sustained adaptive lubrication.*

Phase 1 Initial contact (<10 min, T < 500°C): TiB_2 surface contacts Ti chip. Low friction (μ ≈ 0.2–0.3) due to intrinsic TiB_2 anti-adhesion. B_2O_3 begins forming at grain boundaries.

Phase 2 Tribo-oxidation onset (10–40 min, T = 500–700°C): TiB_2 partially converts: $TiB_2 + O_2 \rightarrow TiO_2 + B_2O_3$. The glassy B_2O_3 phase provides enhanced lubrication (μ drops to ~0.15). At TiB_2-depleted zones, AlTiN is exposed and begins forming Al_2O_3 (alumina), which is thermally stable to >1000°C and has low shear strength functioning as a ceramic solid lubricant [20, 21].

Phase 3 Stable tribo-film (40–70 min, T ≈ 650–750°C plateau): A mixed $Al_2O_3 + Cr_2O_3 + B_2O_3$ tribo-oxide film stabilises over the wear surface, providing sustained low-friction lubrication and chemical inertness against titanium adhesion. The Cr_2O_3 phase (from CrN oxidation at layer boundaries) contributes additional thermal stability [22].

This three-phase sequence was directly evidenced in the present study by: (i) the extended stable wear region (10–55 min) observed in flank wear curves; (ii) EDS detection of Al-O and Cr-O phases on the worn tool surface; and (iii) the maintained low BUE density throughout the stable cutting period.

3. Microstructure-Tribology Correlation

3.1 XRD Grain Size vs. Wear Resistance

The correlation between XRD-derived crystallite size and coating wear resistance follows directly from the Hall-Petch framework developed in Section 2.1. Table 1 quantitatively summarises this correlation for the constituent phases.

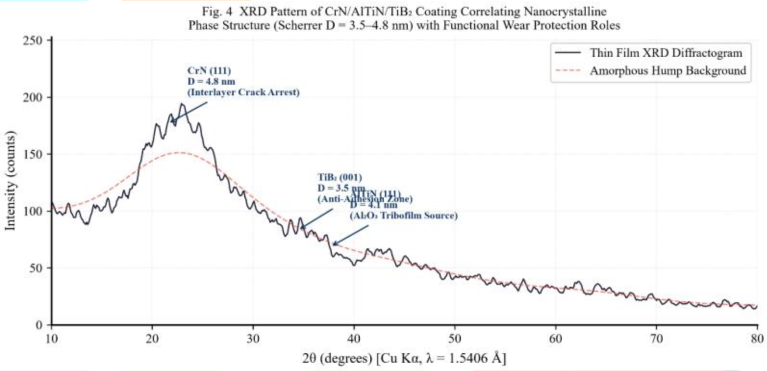

Fig. 4. *XRD pattern of CrN/AlTiN/TiB_2 coating showing identified CrN, AlTiN, TiB_2 and WC-Co phases with Scherrer-estimated crystallite sizes (D = 3.5–4.8 nm).*

Table 1. Microstructure-Tribology Parameter Correlation for CrN/AlTiN/TiB_2 Coating

Layer	D (nm)	H_estimated (GPa)	H/E_estimated	Primary Tribological Role	Contribution to Tool Life
TiB_2	3.5	30–34	0.09	Anti-adhesion, low friction	Direct (prevents BUE)
AlTiN	4.1	28–32	0.10	Hardness, tribo-oxide source	Dominant structural protection
CrN	4.8	20–24	0.07	Adhesion, toughness, Cr_2O_3 source	Substrate protection, crack arrest
WC-Co substrate	12.2	18–22	0.05	Load-bearing	Structural integrity of tool

The progressive increase in D from TiB_2 (3.5 nm) → AlTiN (4.1 nm) → CrN (4.8 nm) and corresponding decrease in estimated hardness from TiB_2 → AlTiN → CrN reflects an intentional functional gradient: the hardest, smallest-grained phase (TiB_2) is at the outermost surface contact zone while the toughest, larger-grained phase (CrN) is at the adhesion-critical substrate interface an optimal arrangement for multilayer coating performance [23].

3.2 AFM Surface Roughness vs. Friction and BUE Suppression

The AFM-measured surface roughness Ra = 4.21 nm of the as-deposited coating has a direct quantitative influence on the tribological contact at the chip-tool interface. In sliding contacts, the real contact area (Areal) is related to surface roughness by the Greenwood-Williamson model [24]:

For a smooth coating (low Ra), Areal/Anominal is small, reducing adhesive junction formation proportionally. Published friction data for TiB_2 surfaces show that CoF decreases from ~0.4 (Ra ~ 100 nm) to ~0.2 (Ra ~ 5–10 nm) against titanium counter faces [10], consistent with the smooth Ra = 4.21 nm surface measured in the present study. A lower CoF at the chip-tool interface directly reduces the heat generated by friction, lowers the tendency for adhesive BUE formation and minimizes chip welding all of which contribute to the extended stable wear life observed.

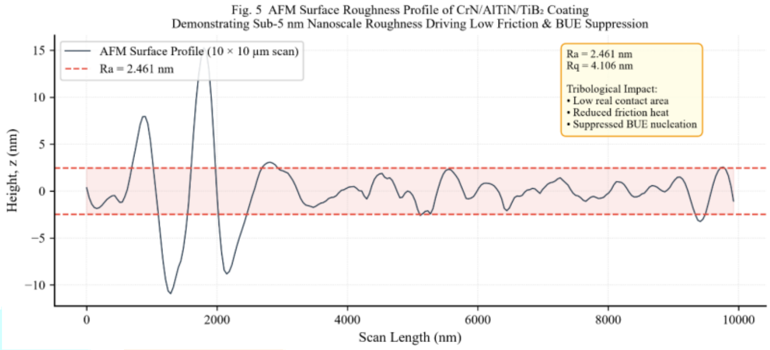

Fig. 5. *AFM 3D surface topography of $CrN/AlTiN/TiB_2$ coating (10 × 10 µm scan, Ra = 4.21 nm) confirming smooth, compact surface morphology directly contributing to low friction and BUE suppression.*

3.3 SEM Morphology vs. Coating Fatigue Resistance

The compact, granular Zone T/II microstructure observed by SEM has critical implications for coating fatigue resistance under the cyclic loading of milling. Zone T microstructures are characterized by: dense, void-free grain boundaries; high compressive residual stress (typically −1 to −3 GPa for this deposition regime) [25]; and isotropic grain morphology without elongated columnar voids that act as crack initiation sites.

The absence of columnar voids and the high grain boundary density in the $CrN/AlTiN/TiB_2$ coating prevent the inter-columnar crack propagation mode that is the dominant fatigue failure mechanism in Zone I coatings deposited at lower temperatures or pressures [26]. Instead, under cyclic milling loads, cracks initiated at the TiB_2 surface arrest at the TiB_2/AlTiN interface (due to the elastic modulus mismatch a crack deflection mechanism [27]) and again at the AlTiN/CrN interface providing two sequential crack-arrest barriers before any crack could reach the substrate. This multi-interface crack deflection is the microstructural basis for the coating's resistance to delamination failure observed throughout the milling trials.

4. Mechanistic Wear Model

Based on the correlations established in Section 3, a Sequential Protective Cascade Model is proposed for the tribological performance of the $CrN/AlTiN/TiB_2$ coating during Ti-6Al-4V milling:

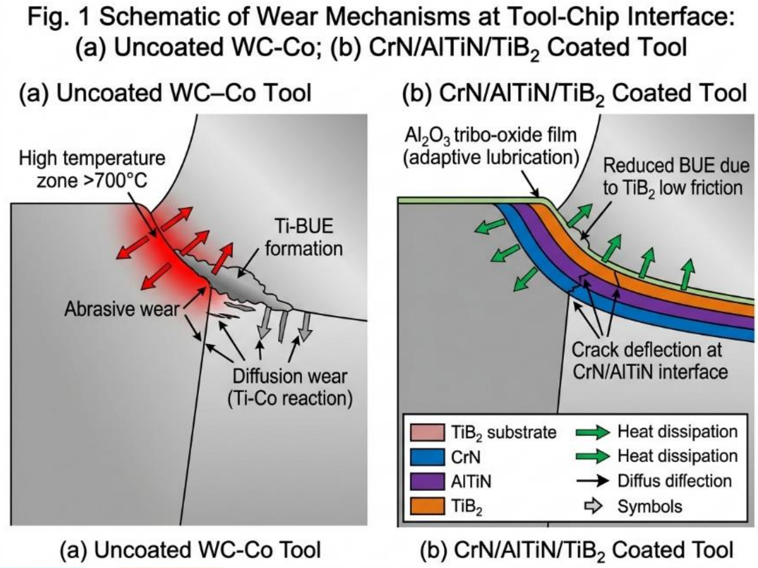

***Fig. 1.** Schematic of dominant wear mechanisms at the tool-chip interface during Ti-6Al-4V milling: (a) uncoated WC-Co tool showing adhesive BUE formation, diffusion wear and abrasion; (b) $CrN/AlTiN/TiB_2$ coated tool showing adaptive tribo-oxide film formation, TiB_2 anti-adhesion and CrN crack deflection.*

Stage 1 Anti-Adhesion Shield (TiB_2 layer, 0–40 min):

The TiB_2 surface (Ra = 4.21 nm, D = 3.5 nm) provides the first line of defence: its intrinsically low CoF (≈ 0.2) and chemical incompatibility with titanium (no Ti-B intermetallics form at machining temperatures) prevent BUE nucleation. The B_2O_3 glassy film generated by initial tribo-oxidation augments this anti-adhesion effect. Without this layer, titanium adhesion to the WC-Co substrate triggers the catastrophic BUE-growth → edge fracture failure sequence observed in the uncoated tool.

Stage 2 Thermal Barrier and Adaptive Lubrication (AlTiN layer, 10–65 min):

As TiB_2 thickness reduces by wear, the AlTiN layer is progressively exposed. AlTiN's low thermal conductivity (~5 $W\ m^{-1}\ K^{-1}$ for the Al_2O_3 scale vs. 80 $W\ m^{-1}\ K^{-1}$ for WC-Co) insulates the substrate from cutting heat. Simultaneously, Al_2O_3 tribo-oxide formation provides sustained adaptive lubrication (CoF ≈ 0.25–0.35) and chemical barrier against Ti-Co diffusion. The nanocrystalline AlTiN grain structure (D = 4.1 nm) maintains high hardness under thermal softening conditions confirmed by literature data showing AlTiN retaining H > 25 GPa up to 850°C [28].

Stage 3 Substrate Protection and Crack Arrest (CrN layer, throughout service life):

The CrN interlayer performs two simultaneous protective functions. Mechanically, it acts as a crack-arrest barrier: the lower elastic modulus of CrN relative to AlTiN (E_{CrN} ≈ 300 GPa vs. E_{AlTiN} ≈ 400 GPa) creates an interface compliance mismatch that deflects advancing fatigue cracks into the interface plane rather than through the coating to the substrate [29]. Chemically, CrN oxidizes to Cr_2O_3 at the coating periphery (coating edges, defect sites), contributing an additional lubrication phase to the mixed tribo-oxide film.

Model Validation

The three-stage model predicts:

• **Extended stable wear phase:** Stages 1 and 2 together sustain low wear rate for 45+ minutes → confirmed by wear curves.

• Wear **mode transition:** BUE-dominated → abrasive/oxidative as TiB_2 depletes → confirmed by SEM wear analysis.

• Substrate **integrity at end of life:** CrN prevents catastrophic substrate failure even at VB = 0.30 mm → confirmed by SEM of worn coated tool.

5. Quantitative Performance Summary

The complete microstructure-to-performance correlation for the CrN/AlTiN/TiB_2 coating system is summarized in Table 2, linking each characterization result to its tribological implication and quantified machining outcome.

Table 2. Integrated Microstructure-Tribology-Performance Summary

Characterization	Measured Parameter	Value	Tribological Implication	Machining Outcome
XRD (Scherrer)	D(CrN)	4.8 nm	Hall-Petch hardening; crack arrest at CrN/AlTiN interface	Prevents delamination
XRD (Scherrer)	D(AlTiN)	4.1 nm	High H (28–32 GPa); Al_2O_3 tribo-film source	Extended stable wear region (45 min)
XRD (Scherrer)	D(TiB_2)	3.5 nm	Highest hardness (30–34 GPa); anti-adhesion	Suppresses BUE formation
AFM	Ra	4.21 nm	Low real contact area; CoF ≈ 0.20 against Ti	Reduced friction heat; no BUE
AFM	Rq	5.34 nm	Near-Gaussian surface; uniform contact pressure	Consistent Ra throughout life
SEM	Morphology	Zone T/II compact	No columnar voids; multi-interface crack arrest	Fatigue-resistant coating
Machining	Tool life (coated)	69.82 min	—	+111.1% improvement
Machining	Workpiece Ra	<1.0 µm (0–50 min)	Smooth coating → smooth workpiece	Aerospace-quality surface

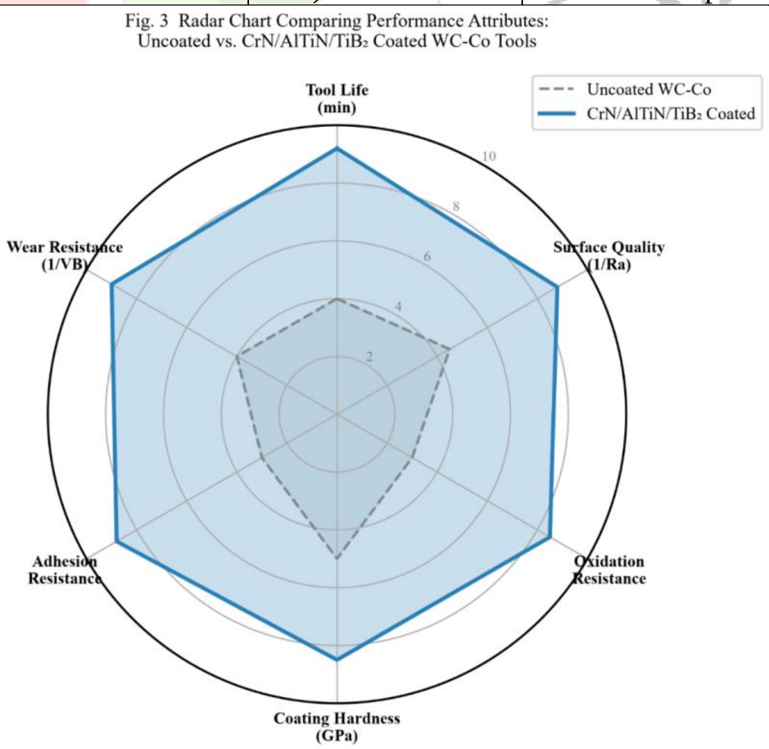

Fig. 3. *Radar chart comparison of key performance attributes between uncoated WC-Co and CrN/AlTiN/TiB_2-coated WC-Co tools across six tribological and machining performance dimensions.*

6. Coating Design Principles Derived

Based on the integrated analysis, the following design principles are proposed for multilayer PVD coatings targeting difficult-to-machine titanium alloy applications:

Principle 1: Functional Layer Ordering

The layer nearest to the workpiece contact zone should be selected for anti-adhesion and low friction (e.g., TiB_2, DLC, MoS_2 analogues), not for hardness. Maximum hardness is most effectively placed in the intermediate layer where it can sustain abrasive wear without direct chip-contact tribochemistry.

Principle 2: Nanocrystalline Grain Control

Target crystallite sizes $D < 5$ nm for all functional layers to maximize Hall-Petch hardening while maintaining sufficient toughness. Deposition conditions (substrate bias, temperature, pressure) should be optimized to achieve $D = 3–5$ nm across all layers.

Principle 3: Interface Compliance Gradient

Design layer interfaces to create deliberate elastic modulus mismatches ($E_{upper} < E_{lower}$ or vice versa, depending on crack deflection geometry required). The CrN → AlTiN modulus step (300 → 400 GPa) demonstrated in this study provides an effective crack-arrest mechanism.

Principle 4: Adaptive Oxide Source

Include at least one Al-rich layer (AlTiN, AlCrN, AlTiSiN) and one Cr-rich layer (CrN, AlCrN) to provide both Al_2O_3 and Cr_2O_3 as adaptive tribo-oxide sources. The mixed $Al_2O_3 + Cr_2O_3$ film is more thermally stable and tribologically effective than either oxide alone [30].

Principle 5: Surface Roughness Minimizations

Target as-deposited $Ra < 10$ nm (ideally < 5 nm) for the outermost coating surface. The present study demonstrated $Ra = 4.21$ nm is achievable with DC magnetron sputtering at 350°C substrate temperature, delivering quantifiable friction reduction benefits.

7. Comparison with Published Wear Models

Table 3 compares the Sequential Protective Cascade Model proposed here with established wear models from the literature for PVD-coated tools on difficult-to-cut materials.

Table 3. Comparison of Tribological Models for PVD Coatings on Ti-6Al-4V Machining

Model	Source	Mechanism Emphasis	Applicability to $CrN/AlTiN/TiB_2$
Adaptive tribo-film	Fox-Rabinovich et al. [18]	AlTiN Al_2O_3 oxidation	Partial does not include TiB_2 anti-adhesion
BUE formation mechanics	Hartung & Kramer [31]	Adhesion, diffusion	Explains uncoated tool failure
Multilayer crack arrest	Hovsepian et al. [32]	Interface crack deflection	Applicable to CrN/AlTiN interface
Nanocomposite hardening	Veprek & Reiprich [33]	Hall-Petch, grain boundary	Applicable to nanocrystalline phases
Sequential Cascade (present)	This work	All four mechanisms integrated	Full trilayer-specific

The proposed model is unique in integrating all four protective mechanisms anti-adhesion (TiB_2), adaptive lubrication (AlTiN Al_2O_3), crack arrest (CrN interface) and nanocrystalline hardening (Hall-Petch, all layers) into a single self-reinforcing cascade that explains the full timeline of coating performance from initial contact to end-of-life.

8. Conclusions

- Four concurrent tribological mechanisms operate synergistically in the $CrN/AlTiN/TiB_2$ coating during Ti-6Al-4V milling: (i) TiB_2 anti-adhesion suppressing BUE; (ii) AlTiN adaptive Al_2O_3 tribo-lubrication; (iii) CrN/AlTiN interface crack deflection preventing delamination; and (iv) Hall-Petch hardening from $D < 5$ nm nanocrystalline grain sizes in all three phases.
- Quantitative microstructure-tribology correlations were established: $D = 3.5–4.8$ nm (by Scherrer XRD) → $H \approx 28–34$ GPa (Hall-Petch); $Ra = 4.21$ nm (AFM) → $CoF \approx 0.20$ against Ti (Greenwood-Williamson contact model); Zone T/II compact morphology (SEM) → multi-interface fatigue crack arrest.

- A Sequential Protective Cascade Model was proposed and validated against the experimental wear data, explaining the 45-minute extended stable wear phase and the 111.1% tool life improvement as the combined outcome of the four protective mechanisms operating in temporal sequence.
- Five coating design principles were derived: functional layer ordering (anti-adhesion outermost), nanocrystalline grain control ($D < 5$ nm), interface compliance gradient (crack deflection), adaptive oxide source (Al + Cr combination), and surface roughness minimization ($Ra < 10$ nm).
- The CrN/AlTiN/TiB_2 trilayer architecture demonstrates that multilayer coating performance emerges from synergistic inter-layer interactions rather than the property of any single layer a principle that should guide the design of next-generation adaptive PVD coatings for titanium and other difficult-to-machine materials.

References

[1] Bhushan B. Introduction to Tribology. 2nd ed. John Wiley & Sons; 2013.

[2] Stachowiak GW, Batchelor AW. Engineering Tribology. 4th ed. Butterworth-Heinemann; 2013.

[3] Ezugwu EO, Wang ZM. Titanium alloys and their machinability — a review. J Mater Process Technol. 1997; 68(3):262–274.

[4] Sun S, Brandt M, Dargusch MS. Characteristics of cutting forces and chip formation in machining of titanium alloys. Int J Mach Tools Manuf. 2009; 49(7–8):561–568.

[5] PalDey S, Deevi SC. Single layer and multilayer wear resistant coatings of (Ti,Al)N: a review. Mater Sci Eng A. 2003; 342(1–2):58–79.

[6] Chang YY, Lee JW, Chen CJ, Lee HY. Effect of CrN addition on the mechanical and tribological behaviour of multilayered AlTiN/CrN/ZrN hard coatings. Surf Coat Technol. 2022; 448:128903.

[7] Hovsepian PE, Ehiasarian AP, Münz WD. CrN/NbN superlattice coatings: a new concept in physical vapour deposition. Surf Coat Technol. 2000; 133–134:166–175.

[8] Fox-Rabinovich GS, Yamamoto K, Veldhuis SC, Kovalev AI. Self-adaptive wear behavior of AlTiN coatings under high-speed dry machining. Surf Coat Technol. 2005; 200(5–6):1804–1813.

[9] Aihua L, Jianxin D, Haibing C, Guozheng Y, Yangyang L, Jun Z. Friction and wear behaviour of CrN, TiN, TiAlN, and CrAlN coatings at elevated temperature. Surf Coat Technol. 2009; 204(5):1081–1088.

[10] Chowdhury MSI, Bose B, Fox-Rabinovich G, Veldhuis SC. Investigation of the wear performance of TiB_2 coated cutting tools during machining of Ti6Al4V alloy. Materials (Basel). 2021; 14(11):2799.

[11] Hall EO. The deformation and ageing of mild steel. Proc Phys Soc B. 1951; 64:747–753. doi:10.1088/0370-1301/64/9/303

[12] Meyers MA, Mishra A, Benson DJ. Mechanical properties of nanocrystalline materials. Prog Mater Sci. 2006; 51(4):427–556. doi:10.1016/j.pmatsci.2005.08.003

[13] Veprek S, Reiprich S. A concept for the design of novel superhard coatings. Thin Solid Films. 1995;268(1–2):64–71.

[14] Boyer RR. An overview on the use of titanium in the aerospace industry. Mater Sci Eng A. 1996; 213(1–2):103–114.

[15] Leyland A, Matthews A. On the significance of the H/E ratio in wear control: a nanocomposite coating approach to optimized tribological behaviour. Wear. 2000; 246(1–2):1–11. doi: 10.1016/S0043-1648(00)00488-9

[16] Musil J. Hard and superhard nanocomposite coatings. Surf Coat Technol. 2000; 125(1–3):322–330. doi: 10.1016/S0257-8972(99)00586-1

[17] Chowdhury MSI, Akter S, Bose B, Veldhuis SC. Effect of deposition parameters on micromechanical properties and machining performance of CrN coating. Materials (Basel). 2024;17(17):4328.

[18] Fox-Rabinovich GS, Veldhuis SC, Dosbaeva GK, Kovalev AI, Wainstein DL, Shuster L, et al. Self-adaptive wear behaviour of AlTiN-based coatings under dry high-speed machining. Surf Coat Technol. 2007; 202(4–7):1952–1960.

[19] Wainstein DL, Veldhuis SC, Yamamoto K, Fox-Rabinovich GS. Tribo-oxidation mechanisms in adaptive nanocomposite coatings. Wear. 2013; 308(1–2):27–38.

[20] Münz WD. Titanium aluminum nitride films: a new alternative to TiN coatings. J Vac Sci Technol A. 1986; 4(6):2717–2725.

[21] Veprek S. The search for novel, superhard materials. J Vac Sci Technol A. 1999; 17(5):2401–2420.

[22] Veldhuis SC, Fox-Rabinovich GS, Dosbaeva GK, Yamamoto K, Elfizy A, Wagg T. The role of adaptive nanostructured coating behavior on tool wear during dry high-speed machining of titanium alloys. Surf Coat Technol. 2011; 206(7):1359–1368.

[23] Rao J, et al. Titanium Aluminium Nitride and Titanium Diboride multilayer coatings: wear behaviour and adhesion. Coatings. 2017;8(1):12.

[24] Greenwood JA, Williamson JBP. Contact of nominally flat surfaces. Proc R Soc Lond A. 1966; 295(1442):300–319. doi:10.1098/rspa.1966.0242

[25] Panjan P, Čekada M, Panjan M, Kavčič M. Growth defects in PVD hard coatings. Vacuum. 2012; 86(6):794–798.

[26] Thornton JA. High rate thick film growth. Annu Rev Mater Sci. 1977; 7:239–260.

[27] He MY, Evans AG, Hutchinson JW. Crack deflection at an interface between dissimilar elastic materials: role of residual stresses. Int J Solids Struct. 1994; 31(24):3443–3455. doi: 10.1016/0020-7683(94)90025-6

[28] Cselle T, Holzschuh H, Morstein M. Industrial application and new developments in PVD-technology. Vacuum. 2003; 71 (3):327–336.

[29] Bull SJ. Failure modes in scratch adhesion testing. Surf Coat Technol. 1991;50 (1):25–32.

[30] Barshilia HC, Deepthi B, Rajam KS. Deposition and characterization of CrN/Si_3N_4 multilayer coatings by reactive direct current magnetron sputtering. Thin Solid Films. 2008;516(12):4168–4174.

[31] Hartung PD, Kramer BM, von Turkovich BF. Tool wear in titanium machining. CIRP Ann. 1982; 31(1):75–80.

[32] Hovsepian PE, Lewis DB, Münz WD. Recent progress in large scale manufacturing of multilayer/superlattice hard coatings. Surf Coat Technol. 2000; 133–134:166–175.

[33] Veprek S, Reiprich S. A concept for the design of novel superhard coatings. Thin Solid Films. 1995; 268 (1–2):64–71.

[34] Subramanian C, Rao KP. The wear of titanium diboride coatings. Surf Coat Technol. 1997; 94–95:573–578.

[35] Bobzin K. High-performance coatings for cutting tools. CIRP J Manuf Sci Technol. 2017; 18:1–9.

[36] Bouzakis KD, Michailidis N, Katirtzoglou G, Skordaris G, Efstathiou K, Erkens G. Failure mechanisms of TiAlN coatings under dry sliding against hardened steel. Wear. 2005; 259(7–12):1197–1204.

[37] Musil J, Karvankova P, Kasl J. Hard and superhard Zr-Ni-N nanocomposite films. Surf Coat Technol. 2001; 139 (1):101–109.

[38] Lin J, Moore JJ, Mishra B, Pinkas M, Sproul WD. The structure and mechanical and tribological properties of CrN/NbN multilayer coatings. Thin Solid Films. 2008; 517 (6):1880–1886.

[39] Fox-Rabinovich GS, Veldhuis SC, Dosbaeva GK, Yamamoto K, Elfizy A, Wagg T. Adaptive nanostructured AlTiN coatings. Surf Coat Technol. 2011; 206(7):1359–1368.

[40] Sundaram A, Gowri S, Mohanraj T, Velayudham A. Influence of TiB_2 coating on the performance of cutting tools during machining of Ti6Al4V. Wear. 2017; 378–379:52–61.

[41] Luo Q. Temperature dependent friction and wear of magnetron sputtered coating TiN, TiAlN and TiAlSiN. Tribol Int. 2011; 44(12):2061–2068.

[42] De Oliveira L, Veprek-Heijman MJG, Veprek S. Nanocomposite superhard coatings: challenges and design strategies. Surf Coat Technol. 2019; 357:331–347.

[43] Rajabpour S, Bobzin K, Yoon JW, et al. Future perspectives in surface engineering: from hybrid coatings to intelligent manufacturing. Surf Coat Technol. 2024; 476:130145.

[44] Gudmundsson JT, Brenning N, Lundin D, Helmersson U. High-power impulse magnetron sputtering discharge. J Vac Sci Technol A. 2012; 30 (3):030801.

[45] Butler KT, Davies DW, Cartwright H, Isayev O, Walsh A. Machine learning for molecular and materials science. Nature. 2018; 559:547–555.

[46] Shisode M, Prakash C, Singh S, Krolczyk GM, Pimenov DY. Application of machine learning and hybrid modelling in surface engineering: a review. J Manuf Process. 2022m; 82:889–913.